Generalized homoclinic solutions and numerical periodicity of the NLS equation

AUTHOR(S):

Umeki, Makoto

CITATION:

Umeki, Makoto. Generalized homoclinic solutions and numerical periodicity of the NLS equation. 数理解析研究所講究録 1996, 974: 21-29

ISSUE DATE:

1996-11

URL:

http://hdl.handle.net/2433/60773

数理解析研究所講究録
974巻 1996年 21-29

NLS方程式のホモクリニック解と数値的周期性

東大理　梅木　誠

Generalized homoclinic solutions and numerical periodicity of the NLS equation

Makoto Umeki
Department of Physics, University of Tokyo

Abstract

A generalization is given of the Ablowitz & Herbst's exact solutions of the nonlinear Schrödinger (NLS) equation, which are temporally homoclinic and periodic in space. It is found that, in numerical simulations of the integrable difference scheme of the NLS equation, periodic and quasi-periodic motions are generated instead of homoclinic orbits. The periods are proportional to $-\ln\epsilon/\Omega_i$, where ϵ is the magnitude of numerical errors and Ω_i is the growth rate of the unstable modes.

Homoclinicity in dynamical systems plays a crucial role in understanding a mechanism of creation of chaos. In low-dimensional systems, it is known as the Melnikov's theorem that a perturbation often destroys the unperturbed homoclinic orbits in integrable systems and create the Smale's horseshoe mapping in the vicinity of them. In this sense, homoclinicity may be regarded as *the fourth route to chaos*, in addition to period-doubling, quasi-periodicity and intermittency. In contrast with low-dimensional systems, the homoclinic structures in higher or infinite dimensions have been studied very recently [1, 3, 4, 6] and the study should be applied to physical phenomena including parametrically forced water waves [7].

On the other hand, the nonlinear Schrödinger equation, which is one of the most-understood integrable equations by soliton theory, is still attractive for study if we consider its periodic boundary problem. In a remarkable paper [1] Ablowitz and Herbst first showed that the focusing nonlinear Schrödinger equation

$$iu_t + u_{xx} + 2\sigma|u|^2u = 0, \tag{1}$$

with $\sigma = 1$ possesses analytically expressed exact solutions which are homoclinic to the periodic solution $u = a\exp 2ia^2t$. The N-homoclinic solution was derived through the transform $x \to ix, t \to -t$ of $2N$-dark-hole soliton solutions of the defocusing nonlinear Schrödinger equation (Eq. (1)

with $\sigma = -1$) with the evenness condition $u(x,t) = u(-x,t)$, which can be derived directly by Hirota's bilinear method. However, we show that the evenness condition is just sufficient but not necessary.

The M-dark-hole soliton solution of the defocusing NLS equation is given by

$$u(x,t) = a\exp(-2ia^2t)g(x,t)/f(x,t), \tag{2}$$

where

$$f(x,t) = \sum_{\tilde{\mu}=0,1} \exp\left[\sum_{j>k}^{M} \alpha_{jk}\mu_j\mu_k + \sum_{j=1}^{M} \mu_j\eta_j\right], \tag{3}$$

$$g(x,t) = \sum_{\tilde{\mu}=0,1} \exp\left[\sum_{j>k}^{M} \alpha_{jk}\mu_j\mu_k + \sum_{j=1}^{M} \mu_j(\eta_j + 2i\phi_j)\right], \tag{4}$$

and

$$\exp(\alpha_{jk}) = \left[\frac{\sin(\phi_j - \phi_k)/2}{\sin(\phi_j + \phi_k)/2}\right]^2 \tag{5}$$

$$\eta_j = p_j(x - x_j) - \Omega_j t + \gamma_j \tag{6}$$

$$p_j = 2a\sin\phi_j \tag{7}$$

$$\Omega_j = \pm p_j\sqrt{4a^2 - p_j^2}, \tag{8}$$

ϕ_j, γ_j and x_j are real constants, $\sum_{\tilde{\mu}=0,1}$ is the summation over all possible combination of $\mu_j = 0$ and 1 for $j = 1,\cdots,M$ and $\sum_{j>k}^{M}$ denotes the summation over all possible pairs chosen from M elements. Here the definition of the phase γ_j is different from that in [1] since we introduced x_j. In order to obtain general homoclinic solutions, we put

$$x = iX, \quad t = -T \quad \text{and} \quad x_j = iX_j. \tag{9}$$

We denote, under the above transform, the relation between the solutions u and U of the defocusing and focusing NLS equations, respectively, as

$$u(x,t;x_j) = U(X,T;X_j). \tag{10}$$

The remaining condition that we should impose is the real-valuedness of $f(x,t)$. This cannot be not satisfied if M is odd, but if M is even, it can be satisfied by letting $p_{2j-1} = -p_{2j}, \gamma_{2j-1} = \gamma_{2j}, \Omega_{2j-1} = \Omega_{2j}, \phi_{2j-1} = \phi_{2j} + \pi$ and $X_{2j-1} = X_{2j}$ for $j = 1,\cdots,N$, where $M = 2N$. This solution gives

not only periodic solutions in space but also quasi-periodic solutions if p_j are incommensurate.

The solution for $N = 1$ is given explicitly by

$$U(X,T) = a\mathrm{e}^{2ia^2T}\frac{1 + 2\cos\varphi\mathrm{e}^{\theta+2i\phi} + A_{12}\mathrm{e}^{2\theta+4i\phi}}{1 + 2\cos\varphi\mathrm{e}^{\theta} + A_{12}\mathrm{e}^{2\theta}}, \tag{11}$$

where $\theta = \Omega T + \gamma$, $\varphi = p(X - X_1)$, $p = 2a\sin\phi$ and $A_{12} = \cos^{-2}\phi$, The asymptotic behaviors of $U(X,T)$ as $T \to \pm\infty$ are respectively given by

$$U_- = a\mathrm{e}^{2ia^2T}[1 + 4i\sin\phi\mathrm{e}^{\theta+i\phi}\cos\varphi], \tag{12}$$

$$U_+ = a\mathrm{e}^{2ia^2T+4i\phi}[1 - 4iA_{12}^{-1}\sin\phi\mathrm{e}^{-\theta-i\phi}\cos\varphi]. \tag{13}$$

There is no essential difference between [1] and the present solution for $N = 1$, since the solution is invariant under the translation. If $N = 2$, however, we obtain a family of new solutions

$$U(X,T;X_j) = a\exp(2ia^2T)G(X,T)/F(X,T) \tag{14}$$

where

$$\begin{aligned} G(X,T) \;=\; & 1 + 2\mathrm{e}^{\theta_1+2i\phi_1}\cos\varphi_1 + A_{12}\mathrm{e}^{2\theta_1+4i\phi_1} + 2\mathrm{e}^{\theta_3+2i\phi_3}\cos\varphi_3 \\ & + A_{34}\mathrm{e}^{2\theta_3+4i\phi_3} + 2\mathrm{e}^{\theta_1+\theta_3+2i(\phi_1+\phi_3)}\{A_{13}\cos(\varphi_1+\varphi_3) \\ & + A_{23}\cos(\varphi_1-\varphi_3)\} + 2A_{13}A_{23}A_{34}\mathrm{e}^{\theta_1+2\theta_3+i(2\phi_1+4\phi_3)}\cos\varphi_1 \\ & + 2A_{12}A_{13}A_{23}\mathrm{e}^{2\theta_1+\theta_3+i(4\phi_1+2\phi_3)}\cos\varphi_3 \\ & + A_{12}A_{13}^2A_{23}^2A_{34}\mathrm{e}^{2(\theta_1+\theta_3)+4i(\phi_1+\phi_3)} \end{aligned} \tag{15}$$

and

$$F(X,T) = G(X,T) \quad \text{with} \quad \phi_i = 0 \;\text{ for all } i, \tag{16}$$

where $\theta_i = \Omega_i T + \gamma_i$ and $\varphi_i = p_i(X - X_i)$. We see that there exists necessarily a conjugate counterpart of every complex term in (4) under the transform (9) for arbitrary N, which implies that the real valuedness of f is satisfied. Note that there is a possibility of the application of this solution to the motion of a knotted closed filament.

Next, we show how these homoclinic solutions are affected by numerical errors in simulations. In order to imitate homoclinic orbits numerically as

precise as possible and examine the effect of errors, we perform a following numerical experiment.
1) We adapt the Ablowitz-Ladik system [2]

$$iu_{nt} + (u_{n+1} - 2u_n + u_{n-1})/h^2 + |u_n|^2(u_{n+1} + u_{n-1}) = 0, \qquad (17)$$

which is the integrable finite-difference scheme and does not show any chaotic motions. The number of spatial discretization N_p is taken as 64.
2) We use three numerical codes written in single, double and quadruple precisions, which have about 7, 16 and 33 effective decimal digits of floating point numbers. The truncation error is reduced to the level of the round-off error. For this purpose, we choose as the scheme of time integration the fourth-order Runge-Kutta method in the former two codes, and the sixth-order eight-stage method by Hu$\check{\text{t}}$a[5] in the quadruple case. The temporal steplength Δt is taken as $\Delta t = 10^{-2}, 10^{-3}$ and 10^{-4} so that the local truncation error is roughly estimated as $10^{-8}, 10^{-15}$ and 10^{-28}, which are on a level of the round-off errors. Then, we denote the total size of the local numerical error by ϵ_n
3) The initial conditions are given according to the asymptotic form $T \to -\infty$ of the solution, (12) for $N = 1$. They are expressed by the sum of the fixed point $a\exp(2ia^2T)$ plus a small disturbance which denotes unstable modes. The magnitude of the disturbance is ϵ_n. This may be considered as one of the best implementations of homoclinic orbits in a numerical sense.

First, a 1-homoclinic solution is examined. We put $L = 2\sqrt{2}\pi$ and the initial condition is

$$U(X, T = 0) = 0.5[1 - \epsilon(1 + i)\cos(pX)] \qquad (18)$$

with $p = 2\pi/L$ and $\epsilon = \epsilon_i = \epsilon_n$. The spatio-temporal behavior of $|U|$ in Figure 1 shows not homoclinic but periodic motion in time. We observe the sequence of appearance of bumps, whose positions are fixed or changed alternatively. It should be noted that the periods of three cases are different. The lefi side of Figure 2 shows the temporal evolution of the amplitude $A = \sqrt{|\tilde{U}_1|^2 + |\tilde{U}_{-1}|}$ where the Fourier coefficients $\tilde{U}_j$ is defined by

$$\tilde{U}_j = \frac{1}{N_p}\sum_{l=1}^{N_p} U(X_l)\mathrm{e}^{-ik_jX_l}, \quad X_l = lL/N_p, \quad k_j = 2\pi j/L \qquad (19)$$

The right side of Figure 2 shows the temporal plots of $(\mathrm{Re}(V), \mathrm{Im}(V))$ at $X = 0$, where a new variable $V = U\exp(-2ia^2T)$ is introduced. This periodic motion and its period can be explained as follows.

The initial condition is expressed as

$$V = 0.5 + \epsilon_i \exp(i\varphi_i)\cos(pX). \tag{20}$$

Comparing (12) with (18), we may estimate $\epsilon_i \approx \exp(\Omega T_i + \gamma)$ and

$$T_i = (\ln \epsilon_i - \gamma)/\Omega \tag{21}$$

Similarly, we can estimate the final time T_f of the single bump. The final state may be approximated as

$$V = \exp(4i\phi)[0.5 + \epsilon_f \exp(i\varphi_f)\cos(pX)]. \tag{22}$$

Letting $\epsilon_f \approx \exp[-(\Omega T_f + \gamma)]$, we have

$$T_f = -(\ln \epsilon_f + \gamma)/\Omega \tag{23}$$

Then, the lifetime of the numerical homoclinic solution is

$$T_f - T_c = -(\ln \epsilon_i + \ln \epsilon_n)/\Omega \tag{24}$$

Next, a 2-homoclinic solution is investigated by an initial condition

$$V = 0.5\{1+\epsilon_1 \exp(i\varphi_{i1})\cos[p_1(X-X_1)]+\epsilon_2 \exp(i\varphi_{i2})\cos[p_2(X-X_2)]\}, \tag{25}$$

with $p_1 = 2\pi/L = p_2/2$, $X_1 = 0$, $L = 4\sqrt{2}\pi$ and $\epsilon_1 = \epsilon_2 = 10^{-15}$, $X_2 = 0$ for one case and $\epsilon_1 = \epsilon_2 = 10^{-8}$, $X_2 = \pi/2$ for the other. A doubly-periodic motion is observed numerically instead of the homoclinic solution. Following the above argument on the temporal period, we may estimate the periods between bumps as

$$T_{pi} = -(\ln \epsilon_i + \ln \epsilon_f)/\Omega_i \tag{26}$$

Then, the ratio of the two periods is determined by the ratio of the linear growth rates as

$$\nu = \frac{T_{p2}}{T_{p1}} = \frac{\Omega_1}{\Omega_2}. \tag{27}$$

The present example gives $\Omega_1 = \sqrt{7}/8, \Omega_2 = 1/2$ and $\nu = 0.661$ and the numerically obtained values are $T_{p1} = 84, T_{p2} = 57$ and $\nu = 0.679$. Therefore, the theoretical prediction is confirmed by this numerical simulation.

A generalized homoclinic solution of the NLS equation is given and it is shown that it appears as periodic and quasi-periodic motions in numerical simulations with minimized numerical errors. The dependence of the period on the magnitude of errors may not be restricted to this example but is expected to be applicable to systems having homoclinic structures and small perturbations or noise.

I thank Professor M. J. Ablowitz for his two seminars given in Professor Wadati's group in Department of Physics, University of Tokyo, which motivated me to study this subject.

References

[1] Ablowitz, M. J. and Herbst, B. M., *SIAM J. Appl. Math.* **50**, 339 (1990).

[2] Ablowitz, M. J. and Ladik, J. F., *Stud. in Appl. Math.* **55**, 213 (1976).

[3] Ablowitz, M. J., Schober, C. and Herbst, B. M., *Phys. Rev. Lett.* **71**, 2683 (1993).

[4] Calini, A., Ercolani, N. M., McLaughlin, D. W. and Schober, C. M., *Physica D* **89**, 227 (1996).

[5] Hušta, A., *Acta Fac. Rerum Natur. Univ. Comenian. Math.* **2**, 21 (1957).; Lambert, J. D. *Computational Methods in Ordinary Differential Equations* (John Wiley & Sons, 1973)

[6] McLaughlin, D. W. and Schober C. M., *Physica D*, **57**, 447 (1992).

[7] Umeki, M., *J. Phys. Soc. Jpn.* **60**, 146 (1991).

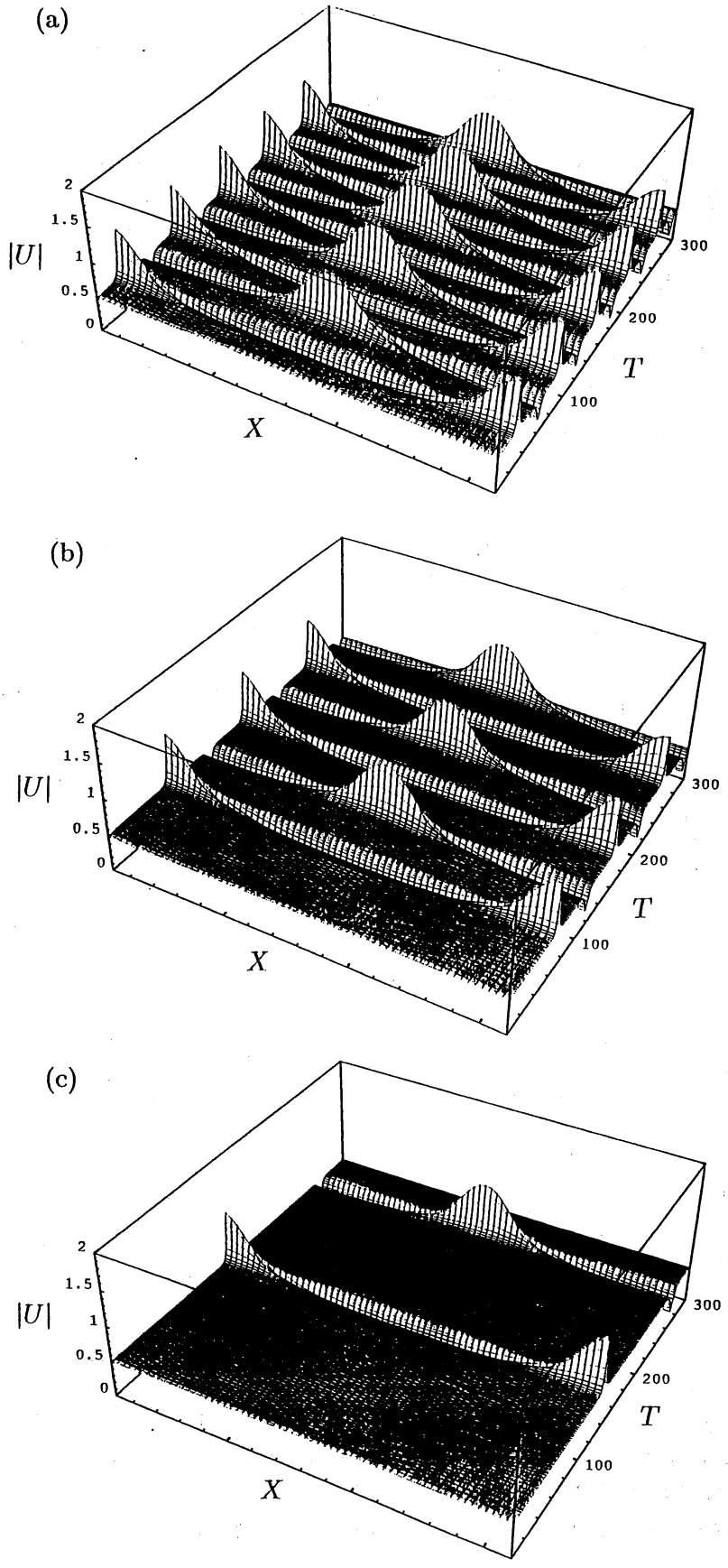

Figure 1. Numerical simulations of the 1-homoclinic solution with (a) single, (b) double and (c) quadruple precisions.

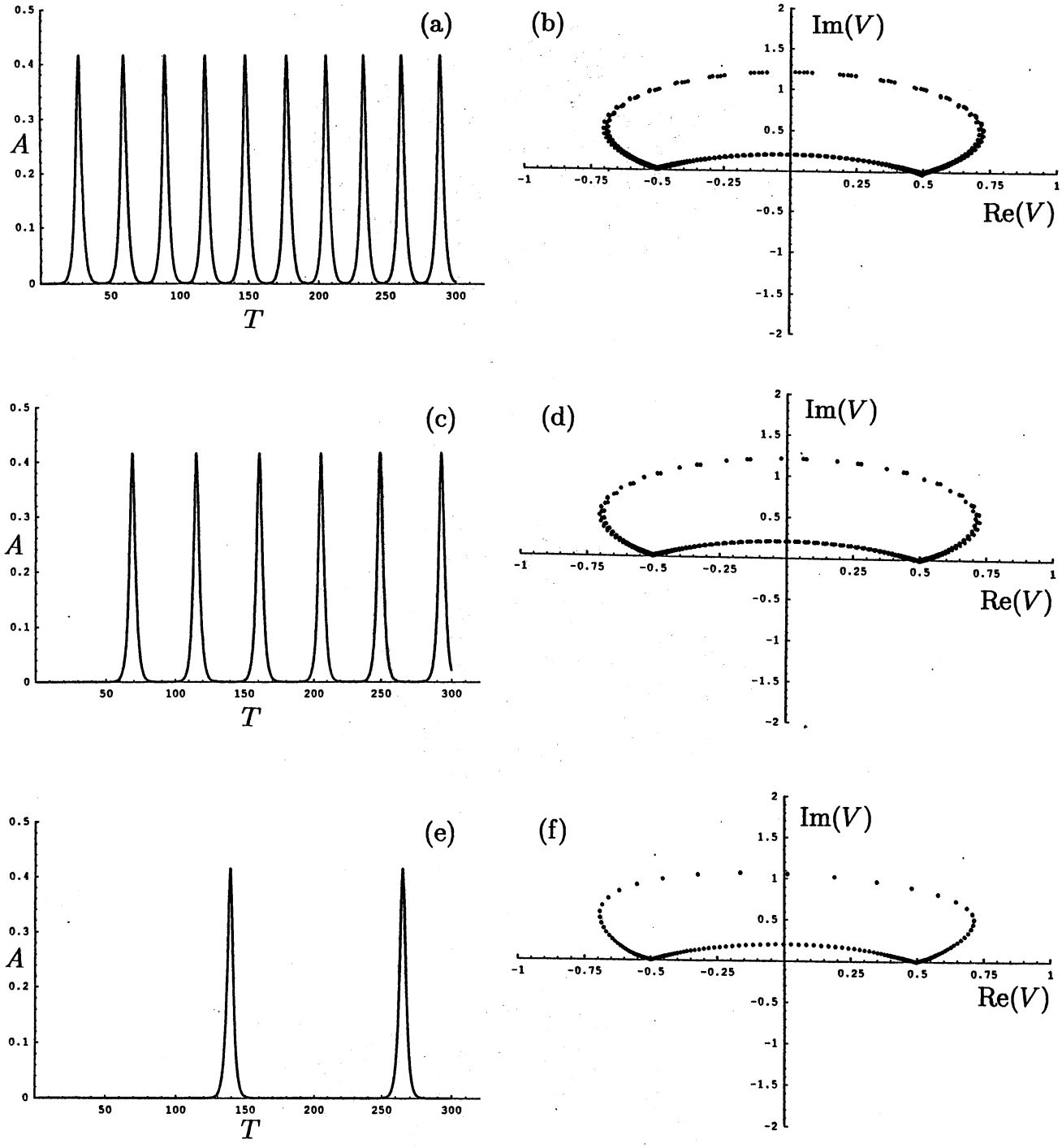

Figure 2. Left: Temporal evolution of the amplitude $A = \sqrt{|\tilde{U}_1|^2 + |\tilde{U}_{-1}|}$ of the spatial Fourier components $\tilde{U}_1$ and $\tilde{U}_{-1}$.
Right: Plots of (Re(V), Im(V)) at $X = 0$.
Precisions are single (a,b), double (c,d) and quadruple (e,f).

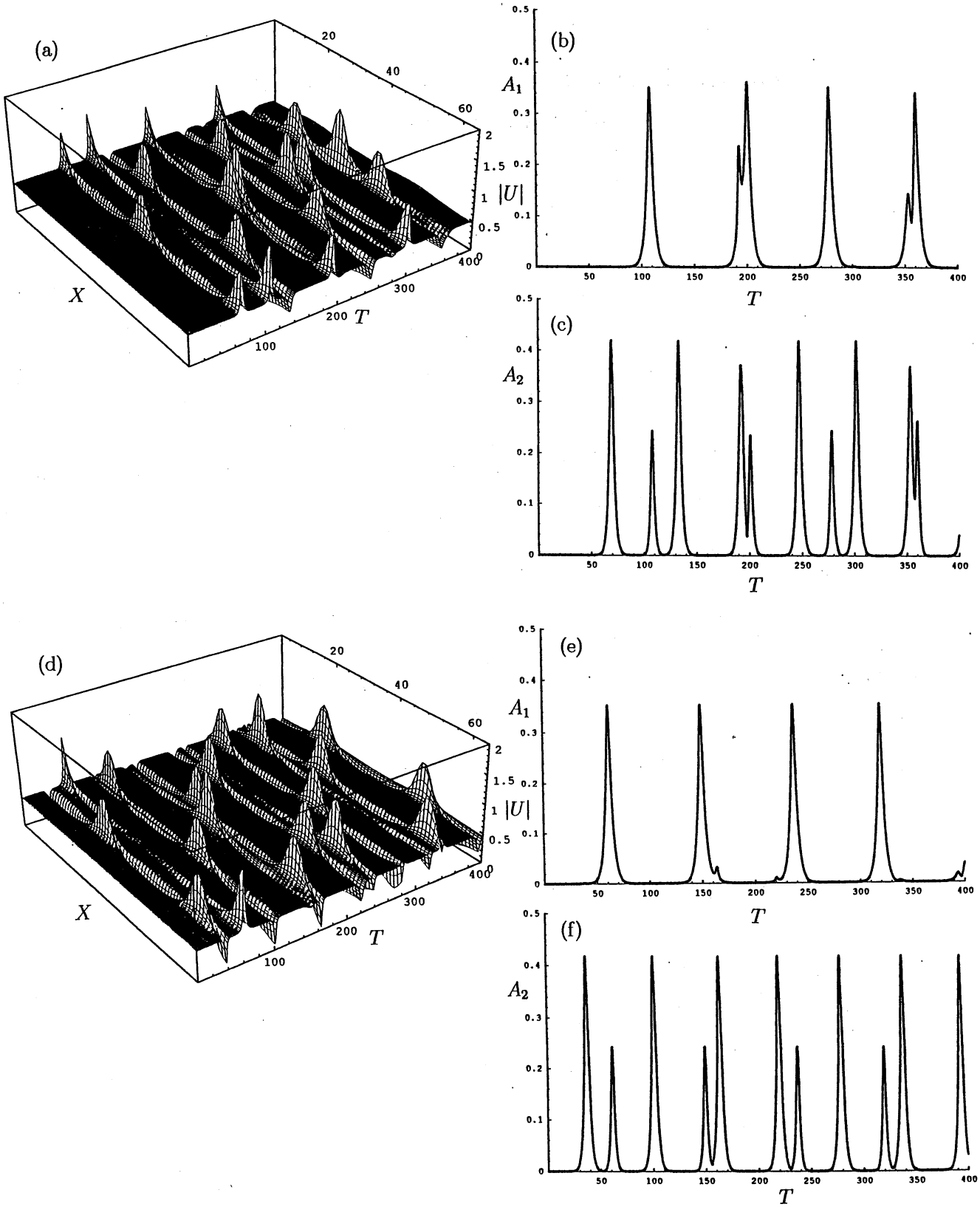

Figure 3. Numerical simulations of the 2-homoclinic solution. Left: Temporal evolution of $|U|$ with double precision. Right: Temporal evolution of $A_1 = \sqrt{|\tilde{U}_1|^2 + |\tilde{U}_{-1}|}$ and $A_2 = \sqrt{|\tilde{U}_2|^2 + |\tilde{U}_{-2}|}$. The initial condition is $U = 0.5[1 + \epsilon e^{i\phi_{01}} \cos p_1 X + \epsilon e^{i\phi_{02}} \cos p_1 (X - X_2)]$, $L = 4\sqrt{2}\pi, p_1 = p_2/2 = 2\pi/L$, and (a-c) $\epsilon = 10^{-15}, X_2 = 0$, (d-f) $\epsilon = 10^{-8}, p_2 X_2 = \pi/2$.